ResearchGate

See discussions, stats, and author profiles for this publication at: https://www.researchgate.net/publication/6746612

Tunable Red−Green Upconversion Luminescence in Novel Transparent Glass Ceramics Containing Er: $NaYF_4$ Nanocrystals

ARTICLE *in* THE JOURNAL OF PHYSICAL CHEMISTRY B · NOVEMBER 2006

Impact Factor: 3.3 · DOI: 10.1021/jp063145m · Source: PubMed

CITATIONS
128

READS
116

5 AUTHORS, INCLUDING:

Daqin Chen
Hangzhou Dianzi University
167 PUBLICATIONS **3,420** CITATIONS
SEE PROFILE

Yunlong Yu
Chinese Academy of Sciences
89 PUBLICATIONS **2,732** CITATIONS
SEE PROFILE

Yuansheng Wang
Chinese Academy of Sciences
160 PUBLICATIONS **4,398** CITATIONS
SEE PROFILE

Available from: Yunlong Yu
Retrieved on: 03 February 2016

Tunable Red-Green Upconversion Luminescence in Novel Transparent Glass Ceramics Containing Er: $NaYF_4$ Nanocrystals

Feng Liu, En Ma, Daqin Chen, Yunlong Yu, and Yuansheng Wang*

State Key Laboratory of Structural Chemistry, Fujian Institute of Research on the Structure of Matter, Chinese Academy of Sciences, Graduate School of Chinese Academy of Sciences, Fuzhou, Fujian 350002, China

Received: May 23, 2006; In Final Form: August 22, 2006

To develop $NaYF_4$ as bulk luminescence material, transparent glass ceramics containing Er^{3+}: $NaYF_4$ nanocrystals were fabricated for the first time, and the influences of heat-treatment temperature and Er^{3+} doping level on their upconversion luminescence were investigated. With increasing heating temperature, the upconversion intensity enhanced accordingly, attributing to the incorporation of more Er^{3+} into the grown $NaYF_4$. Notably, when the heating temperature reached 650 °C, the upconversion intensity augmented drastically due to the occurrence of phase transition from the cubic $NaYF_4$ to the hexagonal one. Interestingly, for the samples heat-treated at 620 °C, when the Er^{3+} doping level was increased from 0.05 to 2.0 mol %, the upconversion emission was whole-range tunable from monochromatic green to approximately monochromatic red, which could be mainly attributed to the cross-relaxation between Er^{3+} ions. The excellent optical properties and its convenient, low-cost synthesis of the present glass ceramic imply that it is an excellent substitution material for the unobtainable bulk $NaYF_4$ crystal, potentially applicable in many fields.

1. Introduction

Recently, much attention has been paid to the study of upconversion (UC) phosphors, which emit higher energy photons via absorbance of lower energy exciting photons. Since the high-power NIR pump lasers are easily obtainable, efficient NIR-to-visible upconversion luminescence of UC phosphors is expected to play a significant role in the field of display technology. Nowadays, UC phosphors have been applied in many fields such as solid-state lasers,[1] NIR quantum counting devices,[2] and fluorescence labels for sensitive detection of biomolecules.[3] Recently, Shalav et al. reported that the efficiency of the silicon solar cells could be enhanced via the application of UC phosphors.[4]

Many rare-earth doped fluoride-based phosphors possess the UC ability for their low phonon energy. Among them, $NaYF_4$ crystal doped with Er^{3+}, Yb^{3+} is known as one of the most efficient NIR-to-visible UC hosts; its visible emission is at least 2 times greater than that of YF_3: Er^{3+}, Yb^{3+} under optimum excitation.[5] Inspired by the fascinating properties of $NaYF_4$, many works have been dedicated to its manufacture: Menyuk et al. synthesized the $NaYF_4$ powders for the first time in 1972.[5] Kano et al. reported subsequently the fabrication of hexagonal $NaYF_4$.[6] Due to the existence of transition between cubic and hexagonal phases, $NaYF_4$ cannot be readily grown as bulk single crystal;[7] thus, most of the attention has been focused on the $NaYF_4$ powders in past years.[8−12] However, there are some restrictions for powder $NaYF_4$ in the application fields such as solid-state laser and optical amplifiers. To develop $NaYF_4$ as bulk material, the transparent glass ceramic might be an ideal choice. It means growth of $NaYF_4$ nanocrystals through crystallization in the bulk glass matrix with desirable transparency and chemical, mechanical stability. Such transparent glass ceramic containing $NaYF_4$ nanocrystals is expected to exhibit superior spectroscopic properties compared to those of $NaYF_4$ polycrystalline powders due to the reduced adverse light scattering in the luminescence process. In this paper we report for the first time the successful preparation of the transparent glass ceramic containing Er^{3+}: $NaYF_4$ nanocrystals by melt-quenching and subsequent heating, and the effects of heating temperature and doping level of Er^{3+} on its UC luminescence performance.

2. Experimental Section

The precursor glass samples were prepared with the composition in mol % of $40SiO_2$:$25Al_2O_3$:$18NaCO_3$:$10YF_3$:$7NaF$:$xErF_3$ (x = 0.05, 0.2, 0.5, 1.0, and 2.0, respectively). For each batch, about 15 g of original material was fully mixed and melted in a covered platinum crucible in an air atmosphere at 1450 °C for 1 h and then cast into a brass mold followed by annealing at a temperature 100 °C below the glass transition temperature determined by differential scanning calorimetry (DSC) to relinquish the inner stress. The transparent glass samples 4−5 mm in thickness so produced were heat-treated to different temperatures at a rate of 10 K/min, held for 2 h, and then cooled to room temperature naturally to obtain a transparent glass ceramic. Figure 1 shows the photograph of 1% Er^{3+}-doped glass ceramic sample heat-treated at 620 °C for 2 h.

XRD analysis was performed to identify the crystallization phase with a power diffractometer (PANalytical X'Pert Pro) operated at 40 kV and 40 mA, using Cu $K\alpha_1$ as the radiation. The 2θ scan range was 5−85° with a step size of 0.033°. The microstructures of the samples were analyzed by a transmission electron microscope (TEM, JEM-2010) equipped with an energy dispersive spectroscopy (EDS) system. The absorption spectra were measured on a spectrophotometer (Lambda35) with a wavelength range of 200−1000 nm and a resolution of 2.0 nm. The visible upconversion fluorescence signals were detected with InP/InGaAs photomultiplier tubes (PMT, R928) excited by a 30 mW diode laser at 980 nm. All the measurements were carried out at room temperature.

* Corresponding author. Telephone: +86-591-8370-5402. Fax: +86-591-8370-5402. E-mail: yswang@fjirsm.ac.cn.

10.1021/jp063145m CCC: $33.50 © 2006 American Chemical Society
Published on Web 09/28/2006

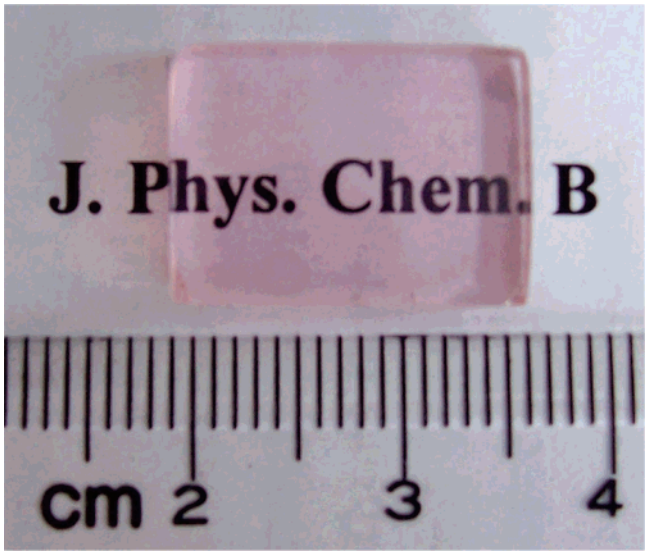

Figure 1. Photograph of 1% Er^{3+}-doped glass ceramic sample heat-treated at 620 °C for 2 h.

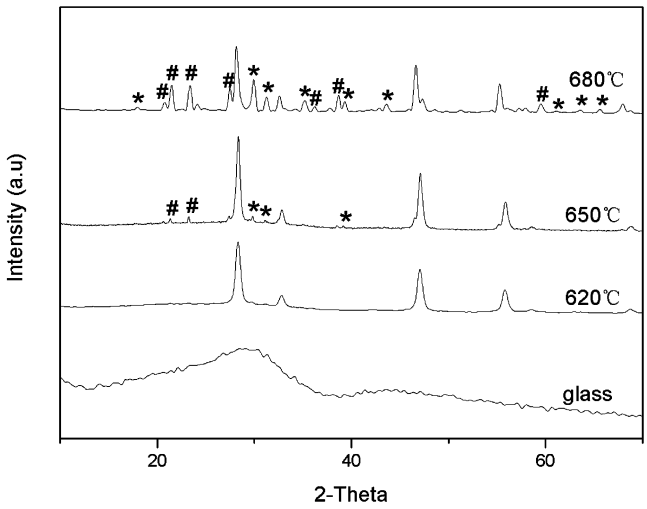

Figure 2. XRD curves of the precursor glass and glass ceramic heat-treated at 620, 650, and 680 °C, respectively. The peaks from β-$NaYF_4$ are indexed by * and those from SiO_2 phase by #. Most of the peaks in the samples heat-treated at 650 and 680 °C are assigned to the cubic α-$NaYF_4$.

3. Results and Discussion

XRD characterizations of glass and glass ceramic were shown in Figure 2. There are only two humps in the XRD curve of the precursor glass sample, indicating its amorphous structure. After heat treatment at 620 °C for 2 h, some intense sharp peaks attributed to cubic α-$NaYF_4$ (JCPDS No. 06-0342) emerge in the XRD curve, indicating the crystallization of α-$NaYF_4$ during thermal treatment. Based on the width of diffraction peaks, the mean grain size calculated by the Debye−Scherrer formula is about 22 nm. With the heating temperature elevated to 650 °C, the volume fraction of α-$NaYF_4$ increased, indicated by the further boost of its diffraction peaks, while a small amount of hexagonal β-$NaYF_4$, which was transformed from α-$NaYF_4$,[3] and SiO_2 phases were formed. Estimated from the integrated diffraction peak intensities, the transformed proportion of α-$NaYF_4$ is about 1%. With further increasing of the temperature to 680 °C, the amounts of β-$NaYF_4$ and SiO_2 phases increased while that of α-$NaYF_4$ decreased, and the sample appeared opaque. According to the phase diagram proposed by Thoma et al.,[13] the hexagonal β-$NaYF_4$ is the thermodynamically stable phase at low temperatures and the cubic α-$NaYF_4$ is the high-temperature modification. In our experiment, since the $NaYF_4$ crystallization process takes place in a metastable glassy system far away from the equilibrium state, the cubic α-$NaYF_4$ phase is obtained as the kinetic product. The transformation from the cubic phase to the hexagonal one is accelerated upon heating, especially when the temperature approaches the eutectic point of 638 °C.

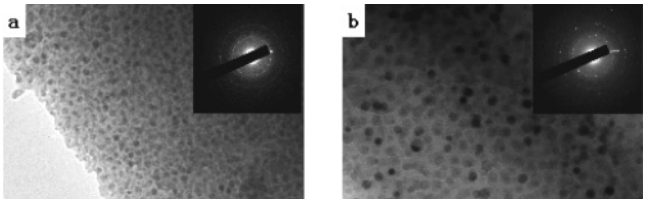

Figure 3. TEM bright field images of glass ceramic heat-treated at (a) 570 °C, 2 h, and (b) 620 °C, 2 h. The insets are the corresponding selected area electron diffraction patterns.

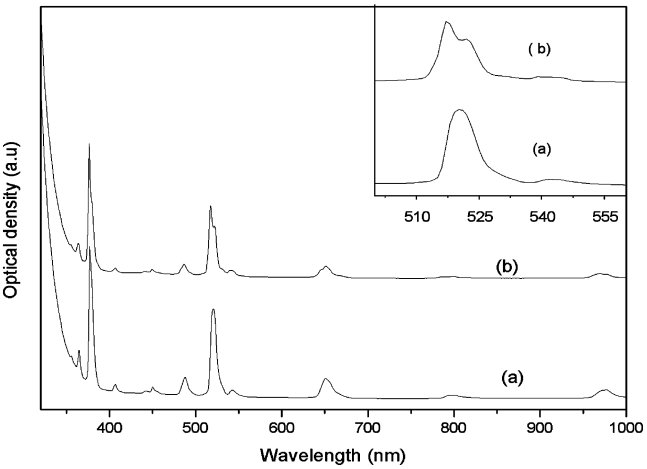

Figure 4. Absorption spectra of (a) the precursor glass and (b) the glass ceramic heat-treated at 620 °C for 2 h. Both samples were doped with 1% Er^{3+}.

TEM micrograph and the corresponding selected area electron diffraction (SAED) pattern of sample heat-treated at 570 °C, given in Figure 3a, indicate spherical crystallites sized 10−15 nm distributed densely and homogeneously in a glass matrix. The crystallites grew to about 20−25 nm when the temperature was raised to 620 °C, as shown in Figure 3b, which coincides well with the XRD analysis. From both XRD and TEM results of a glass ceramic heat-treated at 620 °C, it is notable that the volume fraction of α-$NaYF_4$ is rather high compared to the cases of the transparent oxyfluoride glass ceramics containing PbF_2, LaF_3, or CaF_2 nanocrystals reported previously,[14−16] which might be of benefit for reducing the dilution effect of light emitting for the glass ceramic system. [17]

The absorption spectra of glass and glass ceramic can be used to distinguish the variation of ligand field around rare-earth ions.[18] The absorption spectra of the precursor glass and the glass ceramic heat-treated at 620 °C are shown in Figure 4; both samples were doped with 1.0% Er^{3+}. It is noted that compared to that of the precursor glass, the Stark split and the blue-shift owing to the crystal field effect appear for the 520 nm band of the glass ceramic, which indicate that Er^{3+} ions had incorporated into α-$NaYF_4$. The incorporation of rare-earth

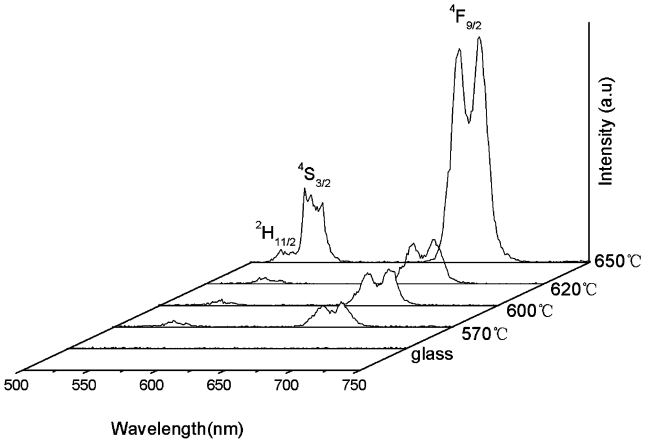

Figure 5. Red and green UC emission of the precursor glass and glass ceramic heat-treated at different temperatures. The emission bands are assigned to the transitions from the indexed levels to $^4I_{15/2}$ level.

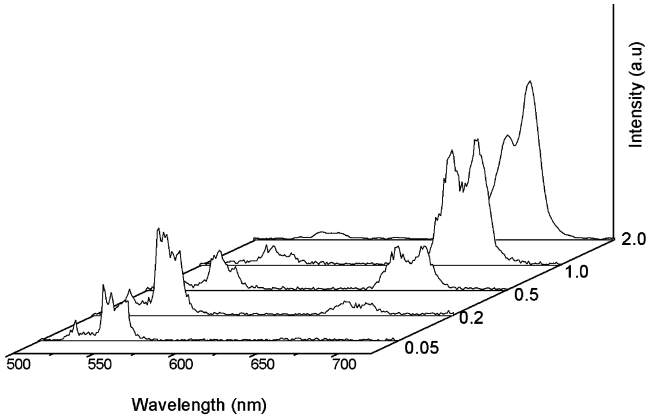

Figure 6. Influence of Er^{3+} concentration on the red and green UC emissions.

ions into the crystalline phase with low phonon energy is a key factor for highly efficient UC luminescence in a glass ceramic system.[19]

To investigate the influence of heating temperature on UC luminescence, the UC emission spectra of 1% Er^{3+}-doped transparent glass ceramic heat-treated at different temperatures were measured under 980 nm excitation, as shown in Figure 5. There was no UC emission for the precursor glass. After the glass was heated at 570 °C for 2 h, along with the emergence of $NaYF_4$ nanocrystals revealed by TEM, considerable green and red UC signals were detected, indicating that the UC luminescence originated only from the part of Er^{3+} in $NaYF_4$ nanocrystals. With increasing heating temperature, the intensities of UC luminescence also increased, implying that more Er^{3+} ions had incorporated into $NaYF_4$ crystalline phase. Notably, when the heating temperature reached 650 °C, the intensities of three UC emission bands assigned to the transitions of $^2H_{11/2} \rightarrow {}^4I_{15/2}$ (520 nm), $^4S_{3/2} \rightarrow {}^4I_{15/2}$ (545 nm), and $^4F_{9/2} \rightarrow {}^4I_{15/2}$ (660 nm), respectively, increased drastically. As was described above, besides α-$NaYF_4$ there were slight β-$NaYF_4$ and SiO_2 crystalline phases emerging in this sample. It is clear that the SiO_2 phase hardly contributed to UC emission owing to its high phonon energy; thus, the drastic enhancement of UC intensity is thought to be attributed mostly to the emergence of the hexagonal β-$NaYF_4$ that had been found having much higher efficiency in UC luminescence than the cubic α-$NaYF_4$.[11] The increased volume fraction of the crystallized α-$NaYF_4$ should be another factor contributing to the enhancement of UC luminescence. It is known that the phase transition from cubic α-$NaYF_4$ to hexagonal β-$NaYF_4$ results in modification of the environment of Y^{3+} occupation sites, including the coordination number.[11,20] According to the study by Aebischer et al.,[21] the much higher UC efficiency of hexagonal β-$NaYF_4$ originated with the interplay of Er^{3+} ions in multiple active sites.

To present a quantitative comparison of the UC emission of Er^{3+} in $NaYF_4$ contained glass ceramic with that in $NaYF_4$ powder, we have synthesized 2.0 mol % Er^{3+}-doped cubic $NaYF_4$ nanocrystalline powder with the mean grain size of about 70 nm by a method reported by Yi et al.[3] and measured its UC emission spectrum with the identical excitation power and wavelength performed for the measurement on the glass ceramic doped with 2.0 mol % Er^{3+}. The spectral distribution of the emission and its intensity of the $NaYF_4$ powder are found quite different from those of the glass ceramic, as shown in the Supporting Information. The overall emission intensity of the glass ceramic is approximately 30 times stronger than that of the $NaYF_4$ nanocrystalline powder, which may benefit from the much weaker light scattering in transparent glass ceramic. The variation in UC intensity induced by phase transition of $NaYF_4$ for different forms of material was also compared. For $NaYF_4$ microcrystalline powder,[11] the intensities of green and green plus red emissions enhanced 10 and 4.4 times, respectively, after the completion of cubic to hexagonal phase transition, while for $NaYF_4$ nanoparticles,[3] the corresponding enhancements reached 40 and 33 times, respectively. Notably, in our glass ceramic system, these augments are 10 and 9 times in the case that only about 1% cubic phase has transformed into the hexagonal one, showing the prominent UC performance of β-$NaYF_4$ in glass ceramic. It is expected that the UC efficiency of the glass ceramic will be much improved when the volume fraction of β-$NaYF_4$ further increases with the prerequisite that the sample maintains good transparency.

The concentration of activation center in the sample plays an important role in luminescence. The UC luminescence spectra of the glass ceramic doped with different contents of Er^{3+} and heat-treated at 620 °C for 2 h were measured, which are presented in Figure 6. Interestingly, the intensity ratio of red to green lights is almost whole range tunable depending on Er^{3+}-doping level: i.e., for the system doped with low content (0.05%) of Er^{3+}, there is only monochromatic green emission; at the medium doping level (0.2−2.0%), with the increase of Er^{3+} content the green emission tends to trail off, while the red one boosts up accordingly; when the content of Er^{3+} reaches 2.0%, the red emission is very intense and the green one nearly disappears. Further increasing of the doping level to 4.0% resulted in similar red to green emission ratio (spectrum not shown). This Er^{3+} concentration dependence of UC emissions could be mainly attributed to the interactions between pairs of Er^{3+} ions.

The possible upconversion mechanism of the investigated system is proposed as depicted in Figure 7. The 4f electrons of Er^{3+} ions at $^4I_{15/2}$ are promoted to $^4I_{11/2}$ through the ground state absorption (GSA) of exciting photons; they are subsequently promoted to the higher levels $^4F_{7/2}$ through excited-state absorption (ESA) and energy transfer upconversion (ETU).[22,23] The absence of UC emission in precursor glass is due to the high phonon energy of oxide glass matrix which leads $^4I_{11/2}$ to be a metastable level; thus, two UC mechanisms referred to above are difficult to achieve. For a system with low Er^{3+} concentration, the green emission preponderating over the red one is owed to the larger energy gap between $^4F_{7/2}$ and $^4F_{9/2}$ levels than that of $^4F_{7/2}$ and $^4S_{3/2}$ levels. Comparatively speaking, the probability of nonradiative decay from $^4F_{7/2}$ to $^4S_{3/2}$ is rather

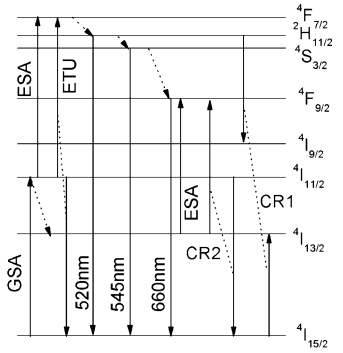

Figure 7. UC luminescence mechanisms of red and green lights.

large, resulting in the dominant population at $^4S_{3/2}$ level responsible for the green emission. The swelling of the green emission at Er^{3+} content under 0.2% is because the interactions between Er^{3+} ions are very weak due to low Er^{3+} concentration; thus, more Er^{3+} ions in nanocrystals could yield higher luminescence intensity. When the concentration of Er^{3+} increased ($\geq$0.2%), the distances between pairs of Er^{3+} ions in $NaYF_4$ reduce correspondingly, which would lead to the near resonant cross relaxation (CR) originating from the interaction of Er^{3+} ions.[24] The intensity quenching of green light might be attributed to the near-perfect resonant CR1: $^2H_{11/2} + {}^4I_{15/2} \rightarrow {}^4I_{9/2} + {}^4I_{13/2}$,[25] as shown in Figure 7. As for the continuous swelling of the red light intensity with the increasing Er^{3+} concentration, a possible mechanism is the cross relaxation of $^4I_{11/2} + {}^4I_{13/2} \rightarrow {}^4F_{9/2} + {}^4I_{15/2}$, denoted as CR2 here, and another mechanism may be owed to the ESA process: $^4I_{13/2}$ + one photon $\rightarrow {}^4F_{9/2}$, as reported in other materials.[26,27]

The great influence of oxide impurities on the upconversion efficiency and the red/green emission distribution of Er^{3+} had been shown for the system of $NaYF_4$ powder.[11] In a complex system as the oxyfluoride glass ceramic the influence of oxides on Er^{3+} upconversion behavior should not be ignored. The Er^{3+} ions in the glass ceramic are divided into two parts, one part incorporates into $NaYF_4$ lattice which generates the UC emission, while the other part remains in the glass matrix which has no contribution to UC emission due to high phonon energy of oxide matrix. For the first part of Er^{3+}, since the $NaYF_4$ nanocrystals are embedded homogeneously in the glassy matrix, those Er^{3+} ions on the near-surface of $NaYF_4$ nanospheres could be regarded as locating partially in the oxide environment and are susceptible to the oxide matrix; thus, their UC efficiency and furthermore the overall UC emission of the sample would be negatively affected. From this point of view, the $NaYF_4$ contained glass ceramic differs from the systems of pure $NaYF_4$ powder or $NaYF_4$ nanoparticles reported previously by others.[3,11] As for the case of changing the Er^{3+} doping level of the $NaYF_4$-contained glass ceramic heat-treated at the same condition (620 °C, 2 h), structurally, the main difference between these samples is the variation of Er^{3+} content in the grains and the glass matrix. The composite structure of the glass ceramic could be regarded basically identical; therefore, the influence of the oxides on Er^{3+} UC emission and red/green color distribution should be roughly the same for all the samples. The change in red/green ratio is thus ascribed mainly to the Er−Er interactions that depend on the doping level.

4. Conclusion

Novel glass ceramics containing Er: $NaYF_4$ nanocrystals with highly efficient upconversion emissions have been developed for the first time. When heated at the temperature near 650 °C, an abrupt enhancement in upconversion emission intensity was observed owing to the occurrence of the phase transition from cubic α-$NaYF_4$ to hexagonal β-$NaYF_4$. For the samples heat-treated at 620 °C, the Er^{3+} concentration has significant influence on the red to green emission ratio that is tunable from monochromatic green to approximately monochromatic red, probably due to the cross relaxation between Er^{3+} ions. This interesting characteristic may enable the device based on Er: $NaYF_4$ glass ceramic to meet the specific color demands, which will have potential applications in the fields of optical display and solid-state laser.

Acknowledgment. This work was supported by the project of Nano-molecular Functional Materials of Fujian Province, China (2005HZ01-1). Helpful comments by the reviewers are appreciated.

Supporting Information Available: The XRD pattern and the UC emission spectrum of the synthesized cubic $NaYF_4$ nanocrystalline powder. This material is available free of charge via the Internet at http://pubs.acs.org.

References and Notes

(1) Downing, E.; Hesselink, L.; Ralston, J.; Macfarlane, R. *Science* **1996**, *273*, 1185.
(2) Chivian, J. S.; Case, W. E.; Eden, D. D. *Appl. Phys. Lett.* **1979**, *35*, 124.
(3) Yi, G.; Lu, H.; Zhao, S. *Nano. Lett.* **2004**, *4*, 2191.
(4) Shalav, A.; Richards, B. S.; Trupke, T.; Krämer, K. W.; Güdel, H. U. *Appl. Phys. Lett.* **2005**, *86*, 013505.
(5) Menyuk, N.; Dwight, K.; Pierce, J. W. *Appl. Phys. Lett.* **1972**, *21*, 159.
(6) Kano, T.; Suzuki, T.; Suzuki, A.; Minagawa, S. *J. Electrochem. Soc.* **1973**, *120*, C87.
(7) Page, R. H.; Schaffers, K. I.; Waide, P. A.; Tassano, J. B. *J. Opt. Soc. Am. B* **1998**, *15*, 996.
(8) Zeng, J.-H.; Su, J.; Li, Z.-H.; Yan, R.-X.; Li, Y.-D. *Adv. Mater.* **2005**, *17*, 2119.
(9) Martin, N.; Boutinaud, P.; Malinowski, M.; Mahiou, R.; Cousseins, J. C. *J. Alloy Compd.* **1998**, *275*−*277*, 304−306.
(10) Heer, S.; Kompe, K.; Gudel, H._U.; Haase, M. *Adv. Mater.* **2004**, *16*, 23.
(11) Krämer, K. W.; Biner, D.; Frei, G.; Güdel, H. U.; Hehlen, M. P.; Lüthl, S. R. *Chem. Mater.* **2004**, *16*, 1244.
(12) Suyver, J. F.; Grimm, J.; van Veen, M. K.; Biner, D.; Krämer, K. W.; Güdel, H. U. *J. Lumin.* **2006**, *117*, 1−12.
(13) Thoma, R. E.; Hebert, G. M.; Insley, H.; Weaver, C. F. *Inorg. Chem.* **1963**, *2*, 1005.
(14) Gouveia-Neto, A. S.; da Costa, E. B.; Bueno, L. A.; Ribeiro, S. J. L. *J. Lumin.* **2004**, *110*, 79−84.
(15) Hu, Z.; Wang, Y.; Bao, F.; Luo, W. *J. Non-Cryst. Solids* **2005**, *351*, 722−728.
(16) Chen, D.; Wang, Y.; Yu, Y.; Ma, E.; Bao, F.; Hu, Z.; Cheng, Y. *Mater. Chem. Phys.* **2006**, *95*, 264−269.
(17) Tashiro, M. *J. Non-Cryst. Solids* **1985**, *73*, 575.
(18) Abril, M.; Méndez-Ramos, J.; Martín, I. R.; Rodríguez-Mendoza, U. R.; Lavín, V.; Delgado-Torres, A.; Rodríguez, V. D. *J. Appl. Phys.* **2004**, *95*, 5271.
(19) Hirao, K.; Tanaka, K.; Makita, M.; Soga, N. *J. Appl. Phys.* **1995**, *78*, 3445.
(20) Mathews, M. D.; Ambekar, B. R.; Tyagi, A. K.; Köhler, J. *J. Alloy Compd.* **2004**, *377*, 162.
(21) Aebischer, A.; Hostettler, M.; Hauser, J.; Krämer, K.; Weber, T.; Güdel, H. U.; Bürgi, H.-B. *Angew. Chem., Int. Ed.* **2006**, *45*, 2802.
(22) Sun, H.; Wen, L.; Duan, Z.; Hu, L.; Zhang, J.; Jiang, Z. *J. Alloy Compd.* **2006**, *414*, 142−145.
(23) Vander Ziel, J. P.; Van Uitert, L. G.; Grodkiewicz, W. H.; Mikulgak, R. M. *J. Appl. Phys.* **1986**, *60*, 4262.
(24) Xu, S.; Yang, Z.; Wang, G.; Dai, S. *J. Alloy Compd.* **2004**, *377*, 253.
(25) De la Rosa-Cruz, E.; Díaz-Torres, L. A.; Rodríguez-Rojas, R. A. *Appl. Phys. Lett.* **2003**, *83*, 4903.
(26) Kumar, G. A.; De la Rosa, E.; Desirena, H. *Opt. Commun.* **2006**, *260*, 60.
(27) Balda, R.; Fernández, J.; Arriandiaga, M. A.; Fdez-Navarro, J. M. *Opt. Mater.* **2004**, *25*, 157.